Published in Plant Molecular Biology, Vol. 81, Issue 1, 2013, p. 13-25
which should be used for any reference to this work

Dual targeting of a mature plastoglobulin/fibrillin fusion protein to chloroplast plastoglobules and thylakoids in transplastomic tobacco plants

Venkatasalam Shanmugabalaji · Céline Besagni · Lucia Eugeni Piller · Veronique Douet · Stephanie Ruf · Ralph Bock · Felix Kessler

Abstract Plastoglobules (PG) are lipid droplets in chloroplasts and other plastid types having important functions in lipid metabolism. Plastoglobulins (PGL) also known as fibrillins (FBN) are evolutionary conserved proteins present at the PG surface but also to various extents at the thylakoid membrane. PGLs are thought to have structural functions in PG formation and maintenance. The targeting of an Arabidopsis PGL (PGL34) to PG required the full protein sequence with the exception of a short C-terminal stretch. This indicated that PGL targeting relies on correct folding rather than a discrete sequence. PGLs lack strongly hydrophic regions and may therefore extrinsically associate with PG and thylakoid membranes via interaction with hydrophilic headgroups of surface lipids. Here, we report on the expression of the Arabidopsis plastoglobulin of 35kD (PGL35 or FBN1a) expressed as a mature protein fused to HIVp24 (human immunodeficiency virus capsid particle p24) or HCV (hepatitis C virus core protein) in transplastomic tobacco. A PGL35–HIVp24 fusion targeted in part to plastoglobules but a larger proportion was recovered in the thylakoid fraction. The findings indicate that transplastomic PGL35–HIVp24 folded correctly after its synthesis inside the chloroplast and then dually targeted to plastoglobules as well as thylakoid membranes.

Keywords Plastid transformation · Plastoglobule · Molecular farming · HIVp24 · HCV core protein · *Nicotiana tabacum*

V. Shanmugabalaji
Department of Plant Biology, University of Geneva,
30, Quai Ernest-Ansermet, 1211 Geneva 4, Switzerland

C. Besagni · L. E. Piller · V. Douet · F. Kessler (✉)
Laboratoire de Physiologie Végétale, Université de Neuchâtel,
Rue Emile-Argand 11, 2000 Neuchâtel, Switzerland
e-mail: felix.kessler@unine.ch

S. Ruf · R. Bock
Max-Planck-Institut für Molekulare Pflanzenphysiologie,
Am Mühlenberg 1, 14476 Potsdam, Golm, Germany

Introduction

Plastoglobules are chloroplast lipid droplets that are attached to thylakoid membranes (Kessler et al. 1999; Austin et al. 2006) and function in diverse aspects of lipid metabolism (Eugeni Piller et al. 2012). The proteome of plastoglobules has around two dozen proteins (Vidi et al. 2006; Ytterberg et al. 2006; Lundquist et al. 2012). These belong to three categories: plastoglobulins/fibrillins (PGL or FBN), plastid metabolic proteins and unclassified proteins. The PGL family in *Arabidopsis* consists of thirteen genes. Seven members were recovered in the plastoglobule proteome. However, it has recently been suggested that plastoglobulin/FBNs partition to varying degrees between the thylakoid membrane and the plastoglobule depending on their respective hydrophocity and isoelectric point (Lundquist et al. 2012). The role of PGLs is probably to control the formation as well as structure and shape of the lipid bodies that have been proposed to "bud" from the thylakoid membrane (Austin et al. 2006). In view of the presence of PGL/FBNs at both PG and thylakoid membranes this may involve their coordinated action at the two compartments. Plastoglobules as well as PGL homologs are present throughout the plant kingdom (Lichtenthaler 1968). Homologues of Arabidopsis PGL35 and PGL34 were notably also

found in the tobacco genome (Pozueta-Romero et al. 1997). It is therefore likely that homologues of Arabidopsis PGLs behave similarly in different species. Previously, we showed that the yellow fluorescent protein fused to PGL34 was expressed and targeted mostly to plastoglobules in nuclear transgenic *Arabidopsis* plants using chloroplast fractionation (Vidi et al. 2007). The study also demonstrated that with the exception of a short C-terminal stretch the complete sequence of a PGL was necessary for proper plastoglobule targeting (Vidi et al. 2007). This finding indicated that correct folding rather than a discrete amino acid sequence is required for assembly of PGLs on PG. The PGLs are encoded in the nucleus, synthesized in the cytoplasm and then imported into the chloroplasts. As import across the chloroplast envelope membrane occurs in an unfolded state of the preprotein, folding must take place after import from the cytosol. Similarly, adipophilin (also termed Adipocyte Differentiation-Related Protein, ADRP), which is a lipid body-associated protein in mammalian cells, has no discrete lipid-binding motif (hydrophobic domains or amphipathic α-helices) and discontinuous stretches of the protein are necessary for targeting to lipid bodies (Targett-Adams et al. 2003). Both PGLs and ADRP lack strongly hydrophobic regions suggesting that they associate extrinsically with the polar headgroups of membrane lipid monolayer surrounding lipid bodies.

Proteins have been targeted to various intra-chloroplast compartments in transplastomic plants. Aprotinin, a bovine protease inhibitor, was targeted to the lumen of thylakoids of tobacco plastid transformants using thylakoid signal peptides derived from nuclear genes which encode luminal proteins (Tissot et al. 2008). Plastid-encoded pre-Tic40 was properly processed and targeted and assembled into a functional complex at the inner membrane of chloroplast (Singh et al. 2008). Zeolin with a plant secretory signal peptide was targeted to the thylakoid membrane upon chloroplast transformation (De Marchis et al. 2011). Recombinant disulfide-bond containing proteins can be expressed in transformed plastids when targeted to the lumen of thylakoids (Bally et al. 2008). But no transplastomic proteins have been targeted to plastoglobules so far.

Here, we express transplastomic PGL/FBN fusion proteins (PGL35–HIVp24 and PGL35–HCV containing a streptavidin tag). Targeting of PGL35–HIVp24 to plastoglobules and thylakoid membranes suggests that the protein folds correctly in the transplastomic system and does not require prior import. PGL35–HIVp24 associated to a considerably higher degree with thylakoids than PG when compared to an endogenous PGL. The endogenous PGL indicated good separation of PG from thylakoids. The different distribution of PGL35–HIVp24 indicated dual targeting to PG and thylakoids in vivo. As the expression level was quite high, this system has potential for application in extrinsic thylakoid membrane and plastoglobule targeting of fusion proteins.

Results

Chloroplast expression constructs

Two tobacco chloroplast transformation DNA constructs pVSB1 and pVSB2 (Fig. 1a) were engineered based on the pZF7lox plastid vector (Zhou et al. 2008). After the initial steps of construction, the coding sequences for the PGL35–HCV core protein and PGL35–HIVp24 were subcloned into the pZF7lox plastid vector by excision and replacement of HIVp24-nef. The expression cassette in pZF7lox is derived from the tobacco plastid Prrn (plastid ribosomal RNA operon) promoter and the 5′UTR of the bacteriophage T7 gene 10 (Kuroda and Maliga 2001). The terminator corresponds to the rbcL 3′ untranslated region (3′UTR). The pZF7lox plastid vector allows homologous recombination with the tobacco plastid genome resulting in insertion between *trnfM* and *trnG* in the large single-copy region of the chloroplast genome. The pZF7lox plastid vector is amenable to the cre-lox system that allows excision of the *loxP (*Locus of crossover in P1) flanked selectable marker gene for streptomycin/spectinomycin resistance (aminoglycoside adenyltransferase; *aadA*) by site-specific recombination using nuclear encoded *CRE* recombinase targeted to plastids (Corneille et al. 2001).

Introduction of transgenes into the tobacco plastid genome

The chloroplast transformation vectors pVSB1 and pVSB2 (Fig. 1a) were introduced into tobacco (*Nicotiana tabacum* cv. Petit Havana) plastids by biolistic transformation (Svab and Maliga 1993). Primary spectinomycin-resistant tobacco lines were selected on regeneration medium of plants (RMOP) containing 500 mg/L spectinomycin. After 4–8 weeks, primary spectinomycin-resistant tobacco lines were obtained. The plastid-transformed (transplastomic) lines were all purified to homoplasmy by carrying out additional regeneration cycles under stringent antibiotic selection. Individual lines were distinguished by an additional number (i.e., 1.1, 1.2 etc.). Several lines isolated from independent transformation events for each construct were characterized in detail. The correct integration of the transgenes into the plastid genome was confirmed by restriction fragment length polymorphism (RFLP) analysis of T_0 plants using Southern blotting. Seeds were obtained from selected T_0 plants. From the resulting T_1 generations, two independently generated transplastomic lines per construct were confirmed by Southern blotting (Fig. 1b). The absence of

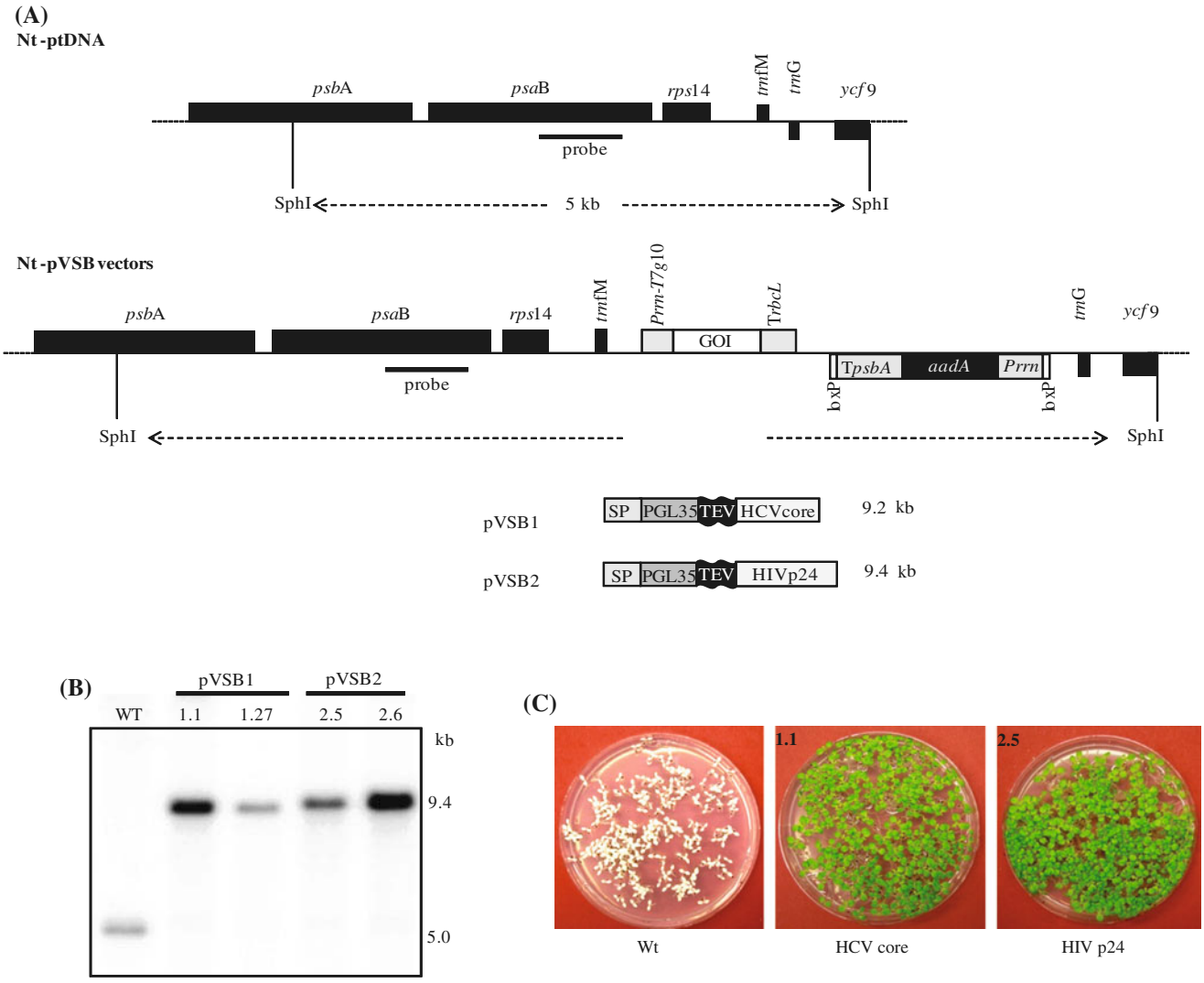

Fig. 1 Engineering of plastid transformants with vectors of the pVSB series. (**a**) Physical map of the targeting region in the plastid genome and structure of plastid transformation vectors of the pVSB series harboring the "genes of interest" (GOI). The GOIs in this study are the coding regions of the vaccine candidates HCV core protein (pVSB1) and HIVp24 (pVSB2). The transgene expression cassette consists of the P*rrn* promoter fused to the 5′ untranslated region (5′UTR) from gene 10 of phage T7 (P*rrn-T7g10*) and the 3′UTR of the plastid *rbcL* gene (T*rbcL*). The transgenes are targeted to the intergenic region between *trnfM* and *trnG*. The chimeric selectable marker gene *aad*A is flanked by loxP sites to facilitate marker excision by the Cre site-specific recombinase. **b** RFLP analysis of tobacco plastid T_1 transformants. Total cellular DNA was digested with *Sph*I and hybridized with probe *psaB* in a Southern blotting experiment (map position shown in Fig. 1a). Data are shown for transplastomic lines transformed with plasmids pVSB1 and pVSB2 and wild-type lines. The fragment size is indicated on the right. Numbering of independently generated transplastomic lines is indicated above each of the lanes (example: 1.1: corresponds to construct pVSB1, line 1). **c** Seed assays to confirm homoplasmy and maternal transgene inheritance. Wild-type seedlings bleach out on spectinomycin-containing medium whereas seedlings from the pVSB1 and pVSB2 transplastomic lines are resistant (*green colour*)

residual copies of the wild-type chloroplast genome from the transplastomic lines revealed that those lines were homoplasmic. In parallel to the RFLP analysis, seed assays to confirm homoplasmy and maternal transgene inheritance were carried out. This is a sensitive way to confirm the homoplasmic state of plastid transformants (Bock 2001). Whereas wild-type seedlings bleach and die on spectinomycin-containing medium, transplastomic seedlings are resistant and indistinguishable from wild-type seedlings grown in the absence of the antibiotic. The homoplasmic lines were 100 % resistant to spectinomycin (Fig. 1c).

Phenotype

pVSB1 and pVSB2 transplastomic lines had wild type phenotypes. To monitor growth and development at different stages, non-transformed wild type and transplastomic lines pVSB1 (1.1) and pVSB2 (2.5) were raised from seeds in

multipurpose compost, without the addition of fertilizer. Initially, plants were grown under defined conditions in a growth room with a 16-h/8-h light/dark cycle for 1 week and then transferred to a greenhouse. The plants developed normally at the seedling stage (Fig. S3a), and also at the age of 4 (Fig. S3b) and 12 weeks (Fig. S3c), apparently having wild-type growth rates and fertility. The chlorophyll fluorescence parameter *F*v/*F*m (maximum photochemical quantum yield of photosystem II) and total chlorophyll content did not differ significantly from the wild type (Table S1). To investigate chloroplast ultrastructure in more detail, we examined chloroplasts in wild type and transplastomic lines by transmission electron microscopy (Fig. 2). Wild type chloroplasts had normal size plastoglobules (approx. 50 nm). In contrast, plastoglobules in both transplastomic lines showed a massive expansion up to around 300 nm.

Expression and quantification of fusion proteins

Northern blot analysis of total RNA from the leaves of pVSB1and pVSB2 derived lines and an untransformed control plant was performed using transgene-specific probes. Hybridization to DNA probes corresponding to the HCV core protein and HIVp24 detected major transcripts with the expected size of 2.7 and 2.9 kb, respectively (Fig. 3a), demonstrating the accumulation of stable mRNAs derived from pVSB1 and pVSB2. Additional, fainter bands were also observed. Although their precise nature is unknown they are most likely derived from the major transplastomic transcripts as they were not detected in the wild type. The upper bands may correspond to dicistronic transcripts whereas the lower bands may be degradation products. Blots stained with methylene blue showing 18S ribosomal RNA bands served as a loading control (Fig. 3a).

SDS-PAGE of total protein extracts followed by Western blot analysis using anti-streptavidin and anti-HIVp24 antibodies confirmed expression of the Streptavidin-PGL35–HIVp24 fusion protein in both pVSB2-derived independent transgenic lines (2.5 and 2.6). A major band at 80 kD was detected in these lines and corresponded to the predicted molecular mass of Streptavidin-PGL35–HIVp24 (Fig. 3b). Streptavidin-PGL35–HCV core fusion protein in transgenic line pVSB1 (1.1) was detected by the anti-streptavidin antibody and gave a band at the expected mass of around 80 kDa. A lower molecular mass band at 44 kDa was also detected (Fig. 3b). The lower molecular mass bands both in pVSB1 and pVSB2 may be due to degradation of the respective fusion proteins. No recombinant protein was detected in samples extracted from wild type control plants. Western blotting using CAB (chlorophyll a/b binding protein) antibodies was used to control for equal loading.

The expression level of Streptavidin-PGL35–HIVp24 fusion protein was quantified by Western blotting using the

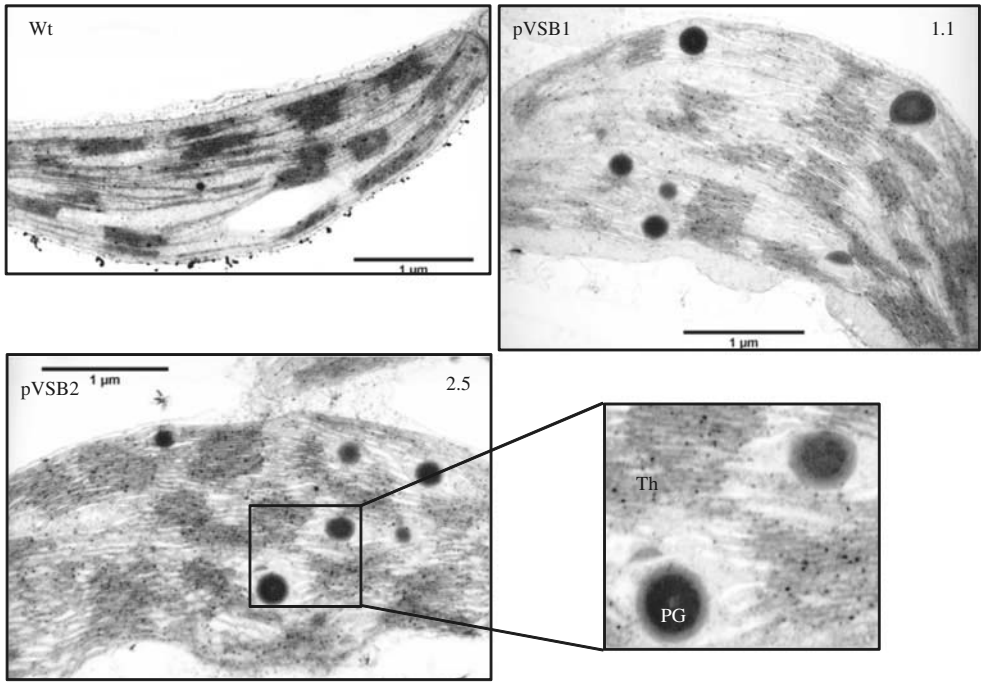

Fig. 2 Ultrastructure of plastoglobules in transplastomic lines. Samples of intact leaf tissue from wild-type and transplastomic lines pVSB1 (1.1) and pVSB2 (2.5) were fixed, stained and observed by transmission electron microscopy. The four panels show chloroplasts from leaf tissue of wild-type and transplastomic lines 1.1 and 2.5. The side panel shows a higher magnification of the boxed region. The positions of the thylakoids (Th) and plastoglobules (PG) are labeled. *Bars* 1.0 µm

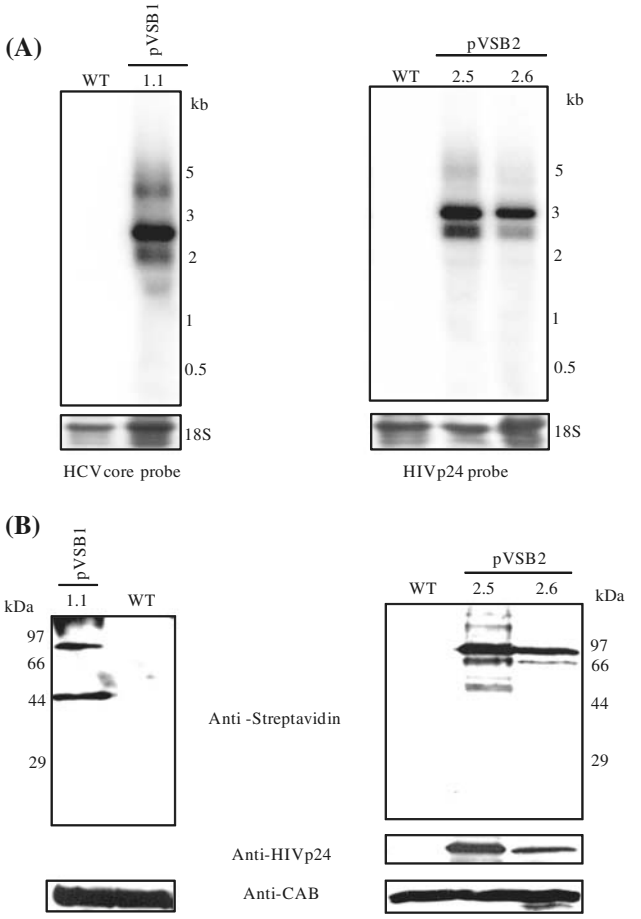

Fig. 3 Expression and recombinant fusion protein accumulation in transplastomic tobacco. **a** Northern analysis of RNA accumulation in pVSB1 (1.1) and pVSB2 (2.5, 2.6) transplastomic tobacco lines. Total cellular RNA was electrophoretically separated, blotted and hybridized to a radiolabelled HCV core protein probe (right) and HIVp24 probe (left). The sizes of the major hybridizing bands in both cases corresponded to the expected size. Methylene blue staining of ribosomal 18S RNA is shown as an RNA loading control. The ssRNA Ladder (NEB N0362S) was used as RNA size marker. **b** Western blot analysis of lines pVSB1 (1.1) and pVSB2 (2.5, 2.6) using anti-STREP, anti-HIVp24 and anti-CAB antibodies. Ten micrograms of total cellular protein were loaded per lane. Anti-CAB antibody (*bottom line*) was used as a loading control

anti-HIVp24 antibody and a dilution series (4, 8 and 12 μg) of total leaf protein extracted from transplastomic line pVSB2 (2.5) (Fig. 4). A dilution series of a total extract of tobacco line pZF5.5A (Zhou et al. 2008) expressing HIVp24 to 4 % of total soluble protein (1, 2 and 3 μg) was used as reference. RbcL is used as a loading control and is weaker in the tobacco line pZF5.5A due to the lesser amount of total protein loaded. (Fig. 4, lower panel). The proportion of total recombinant protein in line pVSB2.5 was estimated to be around 1.0 % of the total protein (Fig. 4). Streptavidin-PGL35–HCV core fusion protein in transgenic line pVSB1 (1.1) was detected using the anti-streptavidin antibody and gave a band of the expected size but of weaker intensity

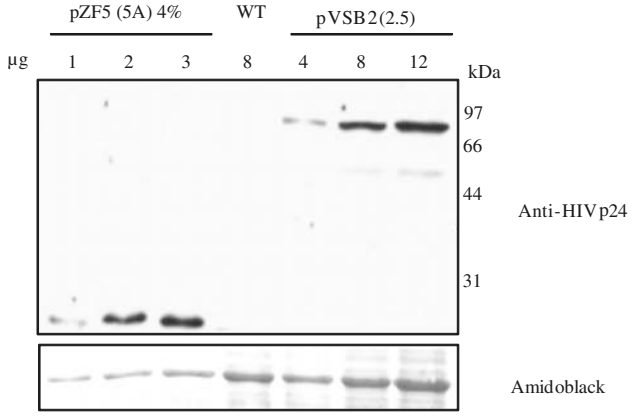

Fig. 4 Western blot analysis for quantification of fusion protein accumulation in transplastomic plants. Total protein extracted from line pVSB2.5 (4, 8 and 12 μg) was used. A dilution series of protein extracted from line pZF5.5A expressing soluble HIVp24 at 4 % of total soluble protein (1, 2 and 3 μg) was used as reference for protein quantification and amidoblack staining of the membrane showing the large subunit of Rubisco (RbcL) was used as a loading control

probably indicating lower levels of expression. For further studies, we only used the pVSB2 (2.5) transplastomic line expressing Streptavidin-PGL35–HIVp24.

Localization of the Streptavidin-PGL35–HIVp24 fusion protein in transplastomic chloroplasts

Chloroplasts were isolated from homoplasmic line 2.5 expressing Streptavidin-PGL35–HIVp24. Immunofluorescence using *Strep*MAB-Immo Oyster 488 gave an intense punctate fluorescence pattern inside chloroplasts (Fig. 5, right panels). This pattern is consistent with plastoglobule localization as well as localization at the thylakoid membranes at and around the points of plastoglobule attachment. The signals observed were specific because no such fluorescence was observed in wild-type chloroplasts (Fig. 5, left panels).

Targeting of the Streptavidin-PGL35–HIVp24 fusion protein to plastoglobules and thylakoid membranes

To determine the distribution of the recombinant fusion protein between plastoglobules and thylakoid membranes, the total chloroplast membrane fractions isolated from WT or pVSB2.5 expressing Streptavidin-PGL35–HIVp24 were subjected to flotation centrifugation on sucrose density gradients (45–5 % sucrose) to separate low-density plastoglobules from higher density envelope and thylakoid membranes. Starting from the top, the gradient was divided into 25 fractions that were separated by SDS-PAGE followed by Western blotting using antisera against PGL40 and CAB as plastoglobule and thylakoid markers, respectively (Fig. 6a, b). The Rubisco large subunit visible in the Amidoblack stained panel (Fig. 6b, asterisk) is a stromal

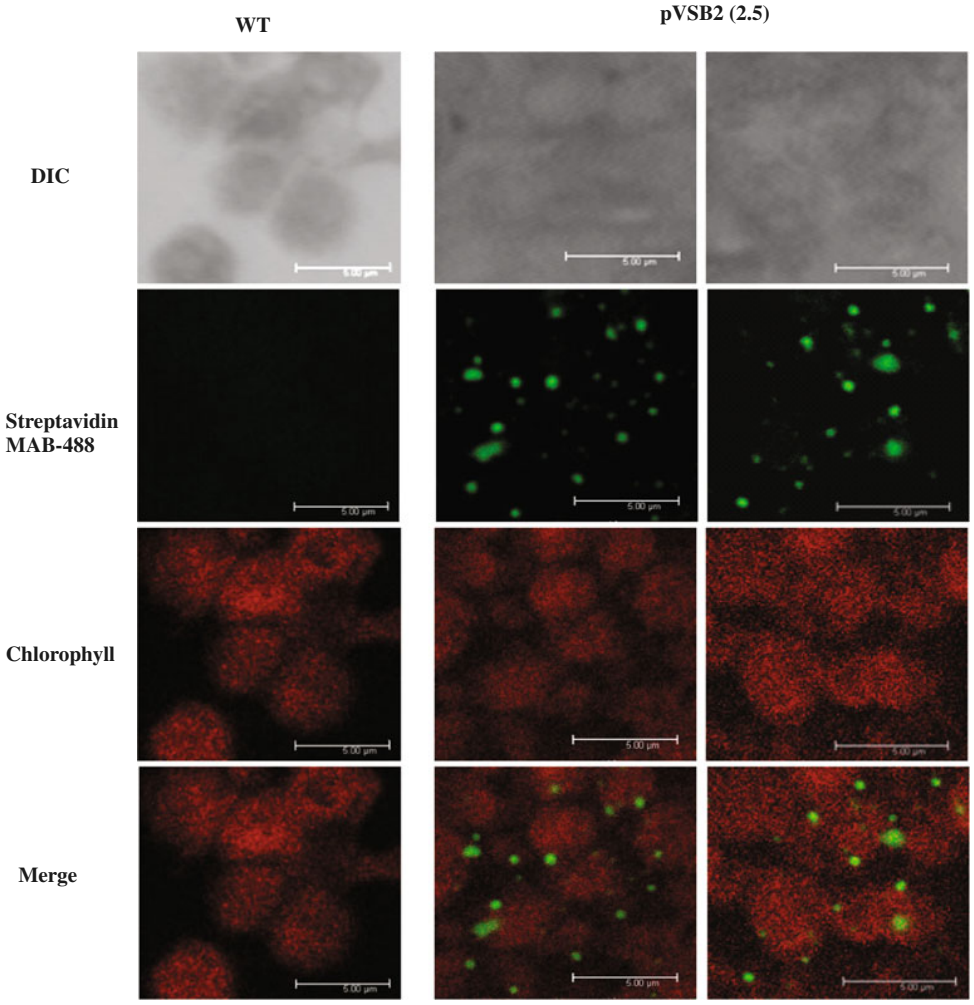

Fig. 5 Localization of Streptavidin-PGL35–HIVp24 in transplastomic chloroplasts. Confocal immunofluorescence microscopic analyses of wild-type and pVSB2 (2.5) chloroplasts. Isolated chloroplasts were decorated with *Strep*MAB-Immo Oyster 488 to detect Streptavidin-PGL35–HIVp24 (*green signal*). Red auto fluorescence (chlorophyll) and the merge of the two signals are also shown. *Bars* 5.0 μm

marker and clearly visible in the heavier fractions but is strongly reduced in the lighter fractions containing plastoglobules. The results demonstrated the separation of plastoglobules (fractions 1–3) from thylakoid membranes (predominantly in fractions 23–25) as well as the removal of the majority of stromal impurity from the plastoglobules (predominantly in fractions 15–25). Streptavidin-PGL35–HIVp24 detected by anti-HIVp24 antibodies, co-distributed with PGL40 (fractions 1–3, 17–25). However, their relative distribution between the fractions was far from identical. The majority of PGL40 was detected in the plastoglobule fractions whereas for Streptavidin-PGL35–HIVp24 the majority was in the thylakoid fractions. To determine the distribution of the recombinant fusion protein resulting from the gradient flotation, the amount of recombinant protein at 5 % sucrose was compared with that at 45 % sucrose by immunoblotting. Around 20 % of the recombinant fusion protein was present in the low-density plastoglobules (5 % sucrose) and around 80 % in high-density thylakoid membranes (45 % sucrose). Five micrograms of isolated plastoglobule protein (pooled fractions 1 to 3 from the gradient) from wild type (WT) and pVSB2.5 were resolved by SDS-PAGE, transferred to nitrocellulose, and immunoblotted with antisera against Streptavidin, HIVP24, PGL30.4 and PGL40 (Fig. 6c). The experiment clearly showed that Streptavidin-PGL35–HIVp24 is present in isolated plastoglobules. CAB (thylakoid marker) and RLSU (large subunit of Rubisco, stromal marker) were not detectable by Western blotting confirming the purity of the plastoglobule fraction.

Purification of HIVp24 using streptavidin–biotin affinity chromatography

To optimize the yield of Streptavidin-PGL35–HIVp24 in the purification procedure, total chloroplasts containing

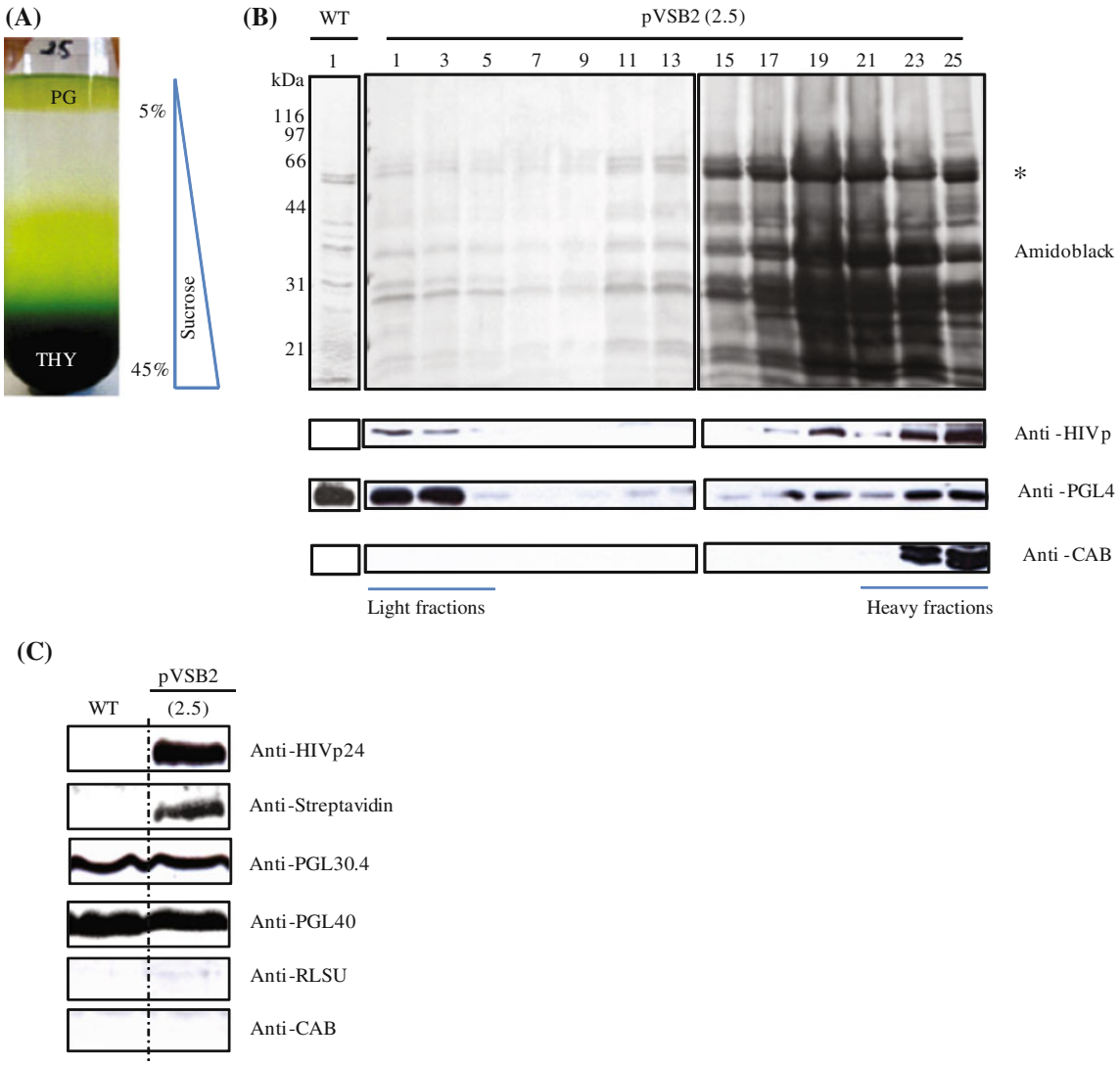

Fig. 6 Purification of recombinant plastoglobules by flotation centrifugation. **a** Total membranes from isolated chloroplasts were separated by flotation on a continuous sucrose gradient. Plastoglobules are visible as a yellowish layer at the top of the gradient. THY, thylakoid membranes; PG, plastoglobules. **b** Western blot analysis of fractions from the density gradient. After ultracentrifugation, 0.5 ml fractions were collected starting from the top of the gradient. Proteins contained in 300 µL of fractions 1–25 were separated by SDS-PAGE, transferred to a nitrocellulose membrane and stained with amidoblack (*upper panel*). Chloroplast fractions from wild type plants (WT) and pVSB2.5 are shown. Antibodies against HIVp24, PGL40 and CAB were used for immuno blotting, as indicated (*lower panels*). The *asterisk* indicates the position of RLSU. **c** Plastoglobules were isolated from total chloroplast membranes of wild type (WT) and pVSB2.5. Five micrograms of plastoglobule protein were resolved by SDS-PAGE, transferred to nitrocellulose, and immunoblotted with antisera to the proteins as indicated. HIVP24, Streptavidin (recombinant protein), PGL30.4, PGL40 (plastoglobule), CAB (thylakoid) and RLSU (stroma)

both the plastoglobules and the thylakoids were solubilized in homogenization buffer containing 1 % Triton-X-100. The solubilisate was separated from insoluble material by centrifugation at 20,000×*g*. The solubilisate was used for affinity purification of Streptavidin-PGL35–HIVp24 using a 2-iminobiotin column. After washing with ammonium carbonate/sodium chloride buffer (pH 11), HIVp24 was eluted from the column by TEV protease cleavage of the bound Streptavidin-PGL35–HIVp24. After TEV (Tobacco etch virus) protease elution, the column was again washed with ammonium carbonate/sodium chloride buffer (pH 11) followed by a final elution step using sodium acetate buffer (pH 4.0). Aliquots retained at each of the steps were subjected to SDS-PAGE separation, transferred to nitrocellulose and stained using amidoblack. The analysis revealed a prominent band in the TEV eluate at the predicted molecular weight of HIVp24 (Fig. 7, upper panel, lane 5). Western blotting using the anti-HIVp24 antibody confirmed

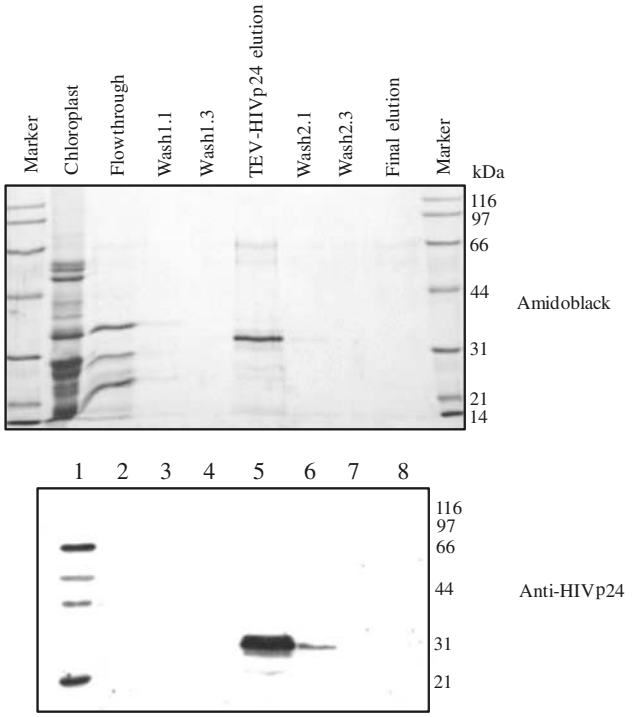

Fig. 7 Purification and analysis of recombinant HIVp24 protein from pVSB2 (2.5) chloroplasts. *Upper panel* Amidoblack-stained nitrocellulose membrane of HIVp24 purification from pVSB2 (2.5) detergent-solubilized chloroplasts using a 2-iminobiotin column for Streptavidin-affinity chromatography. The column was washed repeatedly (*upper panel*, lanes 3 and 4) before TEV elution. Note the major HIVp24 band in the TEV eluate (TEV-HIVp24 elution; lane 5). The column was washed again (*upper panel*, lanes 6 and 7) before Final elution with acidic acetate buffer (*upper panel*, lane 8). *Lower panel* Western-blot analysis of the same nitrocellulose membrane using sheep anti-HIVp24 as the primary antibody

the presence of HIVp24 in the TEV protease eluate (Fig. 7, lower panel).

Discussion

In this work, we examined the expression and targeting of the plastoglobule protein PGL35 mature form fused to either human immunodeficiency virus (HIV) antigen p24 or Hepatitis C virus (HCV) antigen HCV core protein in transplastomic tobacco plants. Arabidopsis PGL35 shares 84 % similarity and 72 % identity with the protein sequence of its closest tobacco homolog (Pozueta-Romero et al. 1997). The PGL35 fusion partners were initially selected for their potential interest as vaccines. HIVp24 is expected to be a key component of an AIDS vaccine (Obregon et al. 2006) and HCV core protein is a target of vaccine development for Hepatitis C disease (Elmowalid et al. 2007). The HIVp24 sequence used here had the additional advantage of being optimized for plastid expression (Zhou et al. 2008).

By visual examination, the transplastomic plants expressing the HIVp24 or the HCV core fusion protein had a wild type phenotype. Moreover, the measured photosynthetic parameters were normal. At the ultra-structural level, transplastomic plastoglobules were enlarged five to sixfold in diameter when compared to the wild type. The mechanisms and significance of variations of plastoglobule size and number are not completely understood. The enlargement of plastoglobules has been described in chloroplasts under abiotic stress, such as drought (Eymery and Rey 1999) and nitrogen starvation (Bondada and Syvertsen 2003). In the case of nitrogen starvation this observation was attributed to chlorophyll degradation and concomitant accumulation of phytylesters in plastoglobules (Gaude et al. 2007). The up-regulation of several plastoglobulin genes also correlated with stress and potentially also correlates with the increase in plastoglobule size (Gillet et al. 1998). Overexpression of a plastoglobulin/fibrillin in tobacco lead to increased clustering of plastoglobules suggesting that plastoglobulins may prevent their coalescing (Rey et al. 2000). Another explanation for the larger size of plastoglobules in transplastomic plants could potentially be an altered partitioning and increased uptake of neutral lipids caused by an imbalance between overexpressed PGL fusion protein and lipid.

The Streptavidin-PGL35–HIVp24 protein, with the codon optimised HIVp24 sequence, accumulated to moderate levels (around 1 %) when compared to other proteins (Tregoning et al. 2003; Glenz et al. 2006). The streptavidin-PGL35–HCV core fusion protein accumulated at lower levels, possibly due to the lack of codon optimization in the HCV coding sequence. The first codons immediately downstream from the AUG start codon have already been identified as an important regulator of translation efficiency in chloroplasts (Kuroda and Maliga 2001). A recent study showed codon optimization of the TGFb3 leading to a 75-fold increase in recombinant protein accumulation relative to the native human coding sequence (Gisby et al. 2011).

The immunofluorescence experiment showed that the recombinant PGL35–HIVp24 fusion protein localized to plastoglobule-like punctate structures inside the chloroplast. In contrast, by membrane fractionation only around 1/5 of the recombinant HIVp24 fusion protein localized to the plastoglobules and much of it was present in the much denser thylakoid fractions. PGL40, a known plastoglobule marker, showed a similar distribution pattern but was much more enriched in the plastoglobule fractions (Fig. 6b) indicating a good separation of plastoglobules from thylakoids. While some plastoglobules may remain attached to the thylakoid membranes during the flotation centrifugation, a proportion of the PGL40 as well as PGL35–HIVp24 are expected to directly associate with the thylakoid membranes (Lundquist et al. 2012). These data could be reconciled with the observed

dot-like immunofluorescence if the PGL35–HIVp24 in thylakoids localizes predominantly to zones where the plastoglobules are attached. A study employing comparative quantitative proteomics of subplastid localization of the Arabidopsis fibrillin family predicts that the distribution of the members between plastoglobule and thylakoids correlates with their hydrophobicity and isoelectric points (Lundquist et al. 2012). In that study, a 34-fold enrichment of PGL35 in plastoglobules over thylakoids was observed. Any fusion partner of PGL35 would change its hydrophobicity and isoelectric point and thereby likely affect its distribution between the thylakoid membranes and the plastoglobules. Indeed, our own calculations demonstrate that the fusion of PGL35 to HIVp24 should shift its distribution towards the thylakoids (Fig. S4). Although plastoglobulins associate with lipid bodies and membranes (Lundquist et al. 2012), their overall amino acid composition is not hydrophobic and it is apparent from hydropathy plots that, unlike oleosin, they lack a strongly hydrophobic structural element. Therefore, association of PGLs with plastoglobules probably involve interactions with the polar head group of membrane lipids at the plastoglobule surface (Kim et al. 2001). Apart from a "bona fide" thylakoid localization, the strong overexpression of PGL35–HIVp24 may saturate the binding sites at the surface of the plastoglobules and force a larger proportion to associate with the thylakoids. By the same token, other PGLs may also see their distribution between the two compartments shifted by the overexpression.

Our previous studies showed that a PGL34 fusion protein containing a chloroplast targeting sequence (transit peptide) was targeted to plastoglobules in nuclear transgenic *Arabidopsis* plants (Vidi et al. 2007). The targeting of a plastome-encoded, mature PGL35-fusion protein to plastoglobules as well as thylakoids demonstrates that the transit peptide of PGL35 is not required for proper assembly. Moreover, it also suggests that plastoglobulin assembly into plastoglobules and thylakoids occurs after import and subsequent folding inside the chloroplast. Based on the findings that hydrophobicity as well as the isoelectric point determine the distribution between plastoglobules and the thylakoids suggests that the net charge and hydrophobic properties at the surface of a folded plastoglobulin may hold the key to understanding the partitioning between the two compartments.

Our construct has an N-terminal streptavidin tag, which has high affinity for 2-iminobiotin (Humbert et al. 2005) and includes three TEV protease sites between PGL35 and HIVp24. We took advantage of these features to purify HIVp24 from a total chloroplast detergent solubilisate using one-step 2-iminobiotin affinity chromatography followed by TEV cleavage to release HIVp24. We used total chloroplasts as the starting material in the purification procedure, because of the association of PGL35–HIVp24 with both the plastoglobule and thylakoid fractions. For this reason also, purification protocols resembling the one in the oleosin system (Vanrooijen and Moloney 1995; Boothe et al. 2010) using a flotation centrifugation step may be inefficient for most plastoglobulin fusion proteins. It is possible however that PGL35 fusion proteins that are more hydrophobic and have a lower isoelectric point may accumulate to a high degree in plastoglobules and be more readily purified by flotation centrifugation.

In conclusion, we demonstrated that a PGL35 fusion protein was dually targeted to plastoglobules as well as to the thylakoid membrane of transplastomic plants. This is in agreement with the recent findings by Lundquist et al. who found that PGL/fibrillins may be distributed to various extents between plastoglobules and thylakoids. A future application for this expression system is therefore the peripheral targeting of PGL-fusion proteins to plastoglobules and thylakoids and to take advantage of the protein enrichment during the chloroplast and total chloroplast membrane purification steps similar to what we show here.

Experimental procedures

Plant material

Aseptically grown tobacco (*N. tabacum* cv. Petit Havana) plants were raised on agar-solidified MS medium (Murashige and Skoog 1962) containing sucrose (30 g/L). Regenerated shoots of transplastomic lines were rooted and propagated on the same media. Rooted homoplasmic plants were transferred to soil and grown to maturity under standard greenhouse conditions.

Transformation of tobacco chloroplasts

Plastid transformation was carried out using the biolistic protocol (Svab et al. 1990). Young leaves from aseptically grown tobacco plants were bombarded with plasmid DNA coated 0.6 μm gold particles using the PDS-1000/He biolistic gun with the Hepta Adaptor (Bio-Rad, Munich, Germany). Primary spectinomycin-resistant lines were selected on a MS-based regeneration medium containing 500 mg/L spectinomycin. Spontaneous spectinomycin-resistant mutants were eliminated by double resistance tests on regeneration medium containing both spectinomycin and streptomycin 500 mg/L each (Bock 2001). For each transgene construct, several independent transplastomic lines were generated and subjected to two to three additional rounds of regeneration on spectinomycin-containing medium to obtain homoplasmic lines. T_0 plants were then transferred to soil and allowed to self-pollinate and set seeds. To determine homoplasmy, T_1 seeds were surface

sterilized and grown on MS-based regeneration medium containing 500 mg/L spectinomycin.

Cloning procedures

The plastid transformation vectors constructed in this study are based on the pZF7lox plastid vector (Zhou et al. 2008). The pZF7lox plastid transformation vectors are derived from plasmids pZSJH1 (Birch-Machin et al. 2004) and pRB95 (Ruf et al. 2001). The plastoglobulin35 (PGL35)-ORF without the coding sequence for the transit peptide gene was amplified from pCL61-PGL35 with PGL35-F forward primer introducing a *Nco*I restriction site at the 5′-end and with PGL35-R reverse primer introducing the coding sequence for three TEV protease sites as well as *Nde*I and *Xba*I restriction sites at the 3′ end. Finally, the amplified product was ligated into the *Nco*I and *Xba*I sites of the pLITMUS28i vector, resulting in pLITMUS28i-PGL35. Coding sequences for Hepatitis C virus antigen-core protein from pSV-sport HCV CE1E2 plasmid (kindly provided by Dr. Bruno Martoglio, Novartis Pharma AG, Basel, Switzerland) was amplified using HCV-F forward primer introducing a *Nde*I restriction site at the 5′ end and with 3′-end HCV-R reverse primer introducing a *Xba*I restriction site. The codon-optimized synthetic HIVp24 (Zhou et al. 2008) from pCR4TOPO-p24 was amplified using the HIVp24-F forward primer introducing a *Nde*I restriction site at the 5′-end and with HIVp24-R reverse primer introducing a *Xba*I restriction at the 3′-end. Both the HCV and HIVp24 amplification products were digested with the *Nde*I and *Xba*I and ligated into the corresponding site of pLITMUS28i-PGL35. The PGL35-HCV core protein and PGL35–HIVp24 fusion genes were amplified from the pLITMUS28i-PGL35 constructs using the PGL35-*Bcl*I forward primer introducing a 5′ *Bcl*I restriction site and HCV-*Bcl*I and HIV-*Bcl*I reverse primers, respectively, introducing a 3′ *Bcl*I restriction site. The amplified product was cloned into pZF7lox plastid transformation vector using the *BamH*I restriction site compatible with *Bcl*I. Finally, the streptavidin tag coding sequence from the pET11b-SAV plasmid was amplified using the Strep-F forward primer and Strep-R reverse primer introducing an *Nco*I restriction site. The amplified product was ligated to the 5′-end of the PGL35–HCV and PGL35–HIVp24 coding sequences in the pZF7lox plastid transformation vector. This resulted in the constructs pVSB1 (*Streptavidin-PGL35:3TEV-HCV core protein*) (Fig. S1a) and pVSB2 (*Streptavidin-PGL35:3TEV-HIVp24*) (Fig. S1b). All steps of the cloning were confirmed by restriction digestion and sequencing.

Southern and northern blot analyses

Total plant DNA was extracted from leaves using the cetyltrimethylammonium bromide (Doyle and Doyle 1990). Five micrograms of total DNA were digested with *Sph*I, separated on a 1 % (w/v) agarose gel and transferred to a Hybond XL membrane (GE Healthcare). A 550 bp PCR product was generated by amplification of a portion of the *psaB* coding region (Wurbs et al. 2007) and was used as RFLP probe to verify plastid transformation and assess the homoplasmic state of the transformants. Probes were labelled with $\alpha[^{32}P]$ dCTP by random priming using the Multiprime DNA labelling system (GE Healthcare). Total cellular RNA was extracted using the peqGOLD TriFast reagent (Peqlab GmbH, Erlangen, Germany) following the manufacturer's protocol. Electrophoretically separated RNA was transferred onto Hybond XL (GE Healthcare) membranes by capillary blotting using standard protocols. Membranes were stained with methylene blue to check the RNA quality and loading. Gene specific probes for the HCV core protein and HIVp24 were amplified by PCR and labelled with $\alpha[^{32}P]$ dCTP by random priming using the Multiprime DNA labelling system (GE Healthcare).

Western blot analysis

Leaves of transformed and untransformed plants grown in a greenhouse were ground in liquid nitrogen. Leaves (100 μg) were homogenized in 250 μL of Rensink buffer (100 mM NaCl, 50 mM Tris–HCl, pH 7.5, 0.5 % (v/v) Triton X-100, and 10 mM β-mercaptoethanol) supplemented with protease inhibitor mixture (Sigma P9599) and centrifuged at $20{,}000 \times g$ for 5 min. Protein was quantified using the Bradford method. Proteins were concentrated by chloroform–methanol precipitation, separated by SDS-PAGE, and blotted onto nitrocellulose membrane. Membranes were stained with amidoblack to check protein quality and control loading. Blots were probed with anti-HIVp24 (sheep anti-p24 antibody; Aalto Bio Reagents, Dublin, Ireland), anti-CAB (Genscript), anti-RLSU (Agrisera), anti-Streptavidin (abcam), anti-PGL40 and anti-PGL30.4 sera (Eurogentec). Detection was performed using the chemiluminescence ECL Western blotting system (GE Healthcare). Quantification of HIVp24 was performed by comparing dilution series of protein extracted from tobacco line pZF5.5A (Zhou et al. 2008). For each sample, adequate amounts were loaded on an SDS-PAGE gel, electrophoretically separated and then analysed by Western blotting. For quantification, chemiluminescent immunoblot signals were analysed using a Bio-Rad ChemiDoc XRS system.

Gradient flotation centrifugation of chloroplast membranes

Leaves from transplastomic and wild-type plants grown on soil for 8 weeks were harvested and immersed in tap water in the dark at 4 °C for 30 min. Leaf material was homogenized in HB buffer (450 mM sorbitol, 20 mM

Tricine/KOH pH 8.4, 10 mM EDTA, 10 mM $NaHCO_3$, 1 mM $MnCl_2$) with a blender and filtered through cheesecloth and Miracloth. Chloroplasts were sedimented (2 min 700×g), washed with HB buffer. The chloroplasts were resuspended in TE buffer (50 mM Tricine/HCl pH 7.5, 2 mM EDTA) containing 0.6 M sucrose and supplemented with 0.5 % (v/v) protease inhibitor cocktail (Sigma P9599) for 10 min. The chloroplasts were lysed by freezing at −20 ∼ for 1 h, thawed on ice, diluted 3 times with TE buffer and homogenised with a Potter homogeniser. Total membranes, corresponding to 10 mg of chlorophyll, were sedimented at 100,000×*g* and resuspended in 2 ml 45 % sucrose in TE buffer. Membranes were overlaid with a linear sucrose gradient created using 15 ml 5 % sucrose and 15 ml of 45 % sucrose in TE buffer and centrifuged for 17 h at 100,000×*g* and 4 °C (SW41Ti rotor, Beckman). 1.2 ml fractions were collected starting from the top of the gradient and used for Western blotting.

Fluorometry and chlorophyll measurement

Maximum quantum efficiency of photosystem II (Fv/Fm) was measured with the Mini-PAM Portable Chlorophyll fluorometer fitted with a 2030-B leaf clip holder (Walz GmbH, Germany). Detached leaves from 6 week-old plants were dark-adapted 15 min prior to measurements. Leaf chlorophyll was quantified in 80 % (v/v) acetone extracts by measuring the A663 and A645 and using the Arnon equations for total chlorophyll content (Arnon 1949).

Electron microscopy

Pieces of leaf tissue from 42-day-old light-grown control and transplastomic plants were fixed with 5 % glutaraldehyde and 4 % formaldehyde in 100 mM phosphate buffer pH 6.8 overnight at 4 °C, rinsed several times in phosphate buffer, and post-fixed for 2 h with 1 % osmium tetroxide in 100 mM phosphate buffer pH 6.8 buffer at 20 °C. After two washing steps in buffer and distilled water, the pieces were dehydrated in ethanol and embedded in Spurr's low-viscosity resin. Ultrathin sections of 50–70 nm were cut with a diamond knife and mounted on uncoated copper grids. The sections were post-stained with uranyl acetate and Reynold's lead citrate. Observations were made with a Philips CM 100 transmission electron microscope (Philips Electron Optics BV, Eindhoven, the Netherlands). For light microscopy, semithin sections with a thickness of 750 nm were cut with a diamond knife, mounted onto glass slides, and stained with toluidine blue.

Immunofluorescence

Chloroplast isolation was performed as previously described (Smith et al. 2002). Chloroplasts were isolated from transplastomic and wild type plants. Isolated chloroplasts were fixed by 2 % paraformaldehyde dissolved in TAN buffer. Fixed chloroplasts were treated by 20 μg/ml proteinase-K in TE buffer containing 0.5 % Triton X-100 at 37 °C for 10 min. Chloroplasts were washed twice with PBS. After blocking with 3 % skim milk in PBS for 30 min, the samples were incubated for 16 h at 4 °C with the anti-streptavidin antibody with *Strep*MAB-Immo Oyster 488 diluted 1:200. Chloroplasts were then washed twice with 3 % skim milk in PBS and then once with PBS buffer (Kabeya et al. 2010). Fluorescence was detected using the FITC (488 nm) laser line from a LEICA TSC SP5 microscope (LEICA Microsystems).

Purification of HIVp24

Leaves from transplastomic plants were harvested and immersed in tap water in the dark at 4 °C for 30 min. Leaf material was homogenized in HB buffer (450 mM sorbitol, 20 mM Tricine/KOH pH 8.4, 10 mM EDTA, 10 mM $NaHCO_3$, 1 mM $MnCl_2$) with a blender and filtered through cheesecloth and Miracloth. Chloroplasts were sedimented (2 min 700 × g), washed with HB buffer. The chloroplasts were resuspended in TE buffer (50 mM Tricine/HCl pH 7.5, 2 mM EDTA) with 0.6 M sucrose supplemented with 0.5 % (v/v) protease inhibitor cocktail (Sigma P9599) and incubated for 10 min. The chloroplasts were lysed by freezing at −20∼ for 1 h, thawed on ice, diluted 3 times with TE buffer and homogenised with a Potter homogeniser. Total membranes, corresponding to 200 μg of chlorophyll, were solubilized with 0.5 % (v/v) Triton X-100 in Rensink buffer (100 mM NaCl, 50 mM Tris–HCl, pH 7.5, 10 mM β-mercaptoethanol) supplied with protease inhibitor mixture (Sigma P9599) at 4 °C for 10 min. The insoluble membranes were sedimented at 20,000 × g and the soluble supernatant was subjected to dialysis in Rensink buffer. The 2-iminobiotin column (Sigma) was washed several times with 50 mM ammonium carbonate at pH 11, containing 0.5 M NaCl. 200 μg of total soluble protein was loaded onto the pre-washed column. After binding, the resin was washed with the same pH 11 buffer until the absorbance of effluent at 280 nm reached base line values. Subsequently, the column was eluted overnight at 4 °C using 100 units of Tobacco Etch Virus Protease (TEV; Invitrogen) in 1 ml of cleavage buffer with 50 mM Tris–HCl, pH 8.0, 0.5 mM EDTA and 1 mM DTT. Then, the column was washed with buffer containing 50 mM ammonium carbonate at pH 11 and 0.5 M NaCl three times. The final elution was carried out using 50 mM sodium acetate pH 4.0 to release streptavidin and was detected by absorbance measurements at 280 nm. Finally, all the fractions were subjected to SDS-PAGE and western blot analysis.

Acknowledgments We thank Stefanie Seeger and Claudia Hasse for help with plant transformation, and the MPI-MP Green Team for plant care and cultivation. We thank Dr. Marc Creus (Department of chemistry, University of Basel) for providing the Streptavidin tag and also Dr. Bruno Martoglio (Novartis Pharma AG, Basel, Switzerland) for providing the HCV core protein cassette. We thank Prof. Jean-Pierre Metraux (University of Fribourg) for kindly making space available in the greenhouse and taking care of the plants. Research in FK's laboratory was supported by the NRP59, the University of Neuchâtel, NCCR "Plant Survival" (National Center of Competence in Research), SystemsX PGCE and the Swiss National Foundation. and UniNe. Work in RB's laboratory was supported by the Max Planck Society and by a grant from the European Union (EU-FP7 METAPRO 244348).

References

Arnon DI (1949) Copper enzymes in isolated chloroplasts—polyphenoloxidase in beta-vulgaris. Plant Phys 24:1–15

Austin JR, Frost E, Vidi PA, Kessler F, Staehelin LA (2006) Plastoglobules are lipoprotein subcompartments of the chloroplast that are permanently coupled to thylakoid membranes and contain biosynthetic enzymes. Plant Cell 18:1693–1703

Bally J, Paget E, Droux M, Job C, Jo D, Dubald M (2008) Both the stroma and thylakoid lumen of tobacco chloroplasts are competent for the formation of disulphide bonds in recombinant proteins. Plant Biotech J 6:46–61

Birch-Machin I, Newell CA, Hibberd JM, Gray JC (2004) Accumulation of rotavirus VP6 protein in chloroplasts of transplastomic tobacco is limited by protein stability. Plant Biotech J 2:261–270

Bock R (2001) Transgenic plastids in basic research and plant biotechnology. J Mol Biol 312:425–438

Bondada BR, Syvertsen JP (2003) Leaf chlorophyll, net gas exchange and chloroplast ultrastructure in citrus leaves of different nitrogen status. Tree Physiol 23:553–559

Boothe J, Nykiforuk C, Shen Y, Zaplachinski S, Szarka S, Kuhlman P, Murray E, Morck D, Moloney MM (2010) Seed-based expression systems for plant molecular farming. Plant Biotech J 8:588–606

Corneille S, Lutz K, Svab Z, Maliga P (2001) Efficient elimination of selectable marker genes from the plastid genome by the CRE-lox site-specific recombination system. Plant J 27:171–178

De Marchis F, Pompa A, Mannucci R, Morosinotto T, Bellucci M (2011) A plant secretory signal peptide targets plastome-encoded recombinant proteins to the thylakoid membrane. Plant Mol Biol 76:427–441

Doyle JJ, Doyle JL (1990) Isolation of plant DNA from fresh tissues. Focus 12:13–15

Elmowalid GA, Qiao M, Jeong SH, Borg BB, Baumert TF, Sapp RK, Hu ZY, Murthy K, Liang TJ (2007) Immunization with hepatitis C virus-like particles results in control of hepatitis C virus infection in chimpanzees. Proc Natl Acad Sci USA 104: 8427–8432

Eugeni Piller L, Abraham M, Dörmann P, Kessler F, Besagni C (2012) Plastid lipid droplets at the crossroads of prenylquinone metabolism. J Ex Bot 63:1609–1618

Eymery F, Rey P (1999) Immunocytolocalization of CDSP 32 and CDSP 34, two chloroplastic drought-induced stress proteins in Solanum tuberosum plants. Plant Physiol Biochem 37:305–312

Gaude N, Brehelin C, Tischendorf G, Kessler F, Dormann P (2007) Nitrogen deficiency in Arabidopsis affects galactolipid composition and gene expression and results in accumulation of fatty acid phytyl esters. Plant J 49:729–739

Gillet B, Beyly A, Peltier G, Rey P (1998) Molecular characterization of CDSP 34, a chloroplastic protein induced by water deficit in Solanum tuberosum L. plants, and regulation of CDSP 34 expression by ABA and high illumination. Plant J 16:257–262

Gisby MF, Mellors P, Madesis P, Ellin M, Laverty H, O'Kane S, Ferguson MWJ, Day A (2011) A synthetic gene increases TGF beta 3 accumulation by 75-fold in tobacco chloroplasts enabling rapid purification and folding into a biologically active molecule. Plant Biotech J 9:618–628

Glenz K, Bouchon B, Stehle T, Wallich R, Simon MM, Warzecha H (2006) Production of a recombinant bacterial lipoprotein in higher plant chloroplasts. Nature Biotech 24:76–77

Humbert N, Zocchi A, Ward TR (2005) Electrophoretic behavior of streptavidin complexed to a biotinylated probe: a functional screening assay for biotin-binding proteins. Electrophoresis 26: 47–52

Kabeya Y, Nakanishi H, Suzuki K, Ichikawa T, Kondou Y, Matsui M, Miyagishima S (2010) The YlmG protein has a conserved function related to the distribution of nucleoids in chloroplasts and cyanobacteria. BMC Plant Biol 10:57

Kessler F, Schnell D, Blobel G (1999) Identification of proteins associated with plastoglobules isolated from pea (*Pisum sativum* L.) chloroplasts. Planta 208:107–113

Kim HU, Wu SSH, Ratnayake C, Huang AHC (2001) Brassica rapa has three genes that encode proteins associated with different neutral lipids in plastids of specific tissues. Plant Physiol 126: 330–341

Kuroda H, Maliga P (2001) Complementarity of the 16S rRNA penultimate stem with sequences downstream of the AUG destabilizes the plastid mRNAs. Nucleic Acids Res 29:970–975

Lichtenthaler HK (1968) Plastoglobuli and fine structure of plastids. Endeavour 27:144–148

Lundquist P, Poliakov A, Bhuiyan NH, Zybailov B, Sun Q, van Wijk KJ (2012) The functional network of the Arabidopsis thaliana plastoglobule proteome based on quantitative proteomics and genome-wide co-expression analysis. Plant Physiol 158: 1172–1192

Murashige T, Skoog F (1962) A revised medium for rapid growth and bio assays with tobacco tissue cultures. Physiol Plant 15: 473–497

Obregon P, Chargelegue D, Drake PMW, Prada A, Nuttall J, Frigerio L, Ma JKC (2006) HIV-1 p24-immunoglobulin fusion molecule: a new strategy for plant-based protein production. Plant Biotech 4:195–207

Pozueta-Romero J, Rafia F, Houlne G, Cheniclet C, Carde JP, Schantz ML, Schantz R (1997) A ubiquitous plant housekeeping gene, PAP, encodes a major protein component of bell pepper chromoplasts. Plant Physiol 115:1185–1194

Rey P, Gillet B, Römer S, Eymery F, Massimino J, Peltier G, Kuntz M (2000) Over-expression of a pepper plastid lipid-associated protein in tobacco leads to changes in plastid ultrastructure and plant development under stress. Plant J 21:483–494

Ruf S, Hermann M, Berger IJ, Carrer H, Bock R (2001) Stable genetic transformation of tomato plastids and expression of a foreign protein in fruit. Nat Biotech 19:870–875

Singh ND, Li M, Lee SB, Schnell D, Daniell H (2008) Arabidopsis Tic40 expression in tobacco chloroplasts results in massive proliferation of the inner envelope membrane and upregulation of associated proteins. Plant Cell 20:3405–3417

Smith MD, Hiltbrunner A, Kessler F, Schnell DJ (2002) The targeting of the atToc159 preprotein receptor to the chloroplast outer membrane is mediated by its GTPase domain and is regulated by GTP. J Cell Biol 159:833–843

Svab Z, Maliga P (1993) High-frequency plastid transformation in tobacco by selection for a chimeric aada gene. Proc Natl Acad Sci USA 90:913–917

Svab Z, Hajdukiewicz P, Maliga P (1990) Stable transformation of plastids in higher-plants. Proc Natl Acad Sci USA 87:8526–8530

Targett-Adams P, Chambers D, Gledhill S, Hope RG, Coy JF, Girod A, McLauchlan J (2003) Live cell analysis and targeting of the lipid droplet-binding adipocyte differentiation-related protein. J Biol Chem 278:15998–16007

Tissot G, Canard H, Nadai M, Martone A, Botterman J, Dubald M (2008) Translocation of aprotinin, a therapeutic protease inhibitor, into the thylakoid lumen of genetically engineered tobacco chloroplasts. Plant Biotech J 6:309–320

Tregoning JS, Nixon P, Kuroda H, Svab Z, Clare S, Bowe F, Fairweather N, Ytterberg J, van Wijk KJ, Dougan G, Maliga P (2003) Expression of tetanus toxin Fragment C in tobacco chloroplasts. Nucleic Acids Res 31:1174–1179

Vanrooijen GJH, Moloney MM (1995) Plant seed oil-bodies as carriers for foreign proteins. Bio Tech 13:72–77

Vidi PA, Kanwischer M, Baginsky S, Austin JR, Csucs G, Dormann P, Kessler F, Brehelin C (2006) Tocopherol cyclase (VTE1) localization and vitamin E accumulation in chloroplast plastoglobule lipoprotein particles. J Biol Chem 281:11225–11234

Vidi PA, Kessler F, Brehelin C (2007) Plastoglobules: a new address for targeting recombinant proteins in the chloroplast. BMC Biotech 7:4

Wurbs D, Ruf S, Bock R (2007) Contained metabolic engineering in tomatoes by expression of carotenoid biosynthesis genes from the plastid genome. Plant J 49:276–288

Ytterberg AJ, Peltier JB, van Wijk KJ (2006) Protein profiling of plastoglobules in chloroplasts and chromoplasts. A surprising site for differential accumulation of metabolic enzymes. Plant Physiol 140:984–997

Zhou F, Badillo-Corona JA, Karcher D, Gonzalez-Rabade N, Piepenburg K, Borchers A-MI, Maloney AP, Kavanagh TA, Gray JC, Bock R (2008) High-level expression of human immunodeficiency virus antigens from the tobacco and tomato plastid genomes. Plant Biotech J 6:897–913